

EXPERIMENTAL INVESTIGATION ON PERALKALINE SILICIC MAGMAS OF PANTELLERIA ISLAND: INFERENCES ON PRE-ERUPTIVE CONDITIONS, AND MAGMA EVOLUTION

PIERANGELO ROMANO

Dipartimento di Scienze della Terra e del Mare Palermo (DiSTeM), Università di Palermo, Via Archirafi, 22, 90123 Palermo

INTRODUCTION

This study focuses on the peralkaline silicic magmatism of Pantelleria Island, Strait of Sicily, Italy. Pantelleria is the emerged portion of a Quaternary volcano located in the Sicily Channel Rift Zone, a domain belonging to African Plate constituted of thinned continental crust. In the petrological literature Pantelleria is well known as the type locality for pantellerite, an iron-rich peralkaline rhyolite. Pantelleria, along its volcanological history, erupted a vast majority of pantellerite and trachyte magmas, and only a small volume of alkali basalts. The debate on the origin of peralkaline silicic magmas dates back to the end of 18th century and nowadays, although numerous advances have been made, some opinion still remain contrasting. In the literature, Pantelleria magmas have been chosen as case study because Pantelleria is one of the best example of peralkaline silicic volcanism in the world and the sole in the Mediterranean area. This project focuses on the petrological aspects of trachytes and pantellerites, exploring with the tools of experimental petrology two principal aspects: *i*) pre-eruptive temperature, pressure, redox conditions of the peralkaline magmas erupted during some key eruptions, and *ii*) the origin of peralkaline rock from a metaluminous parental magma.

More in detail this experimental study has several targets: *i*) to establish the pre-eruptive conditions of trachytic magma of Pantelleria erupted during two very different eruptions, *i.e.*, the upper member of the plinian Green Tuff (GT) eruption (age 45 ka) and the lava flow that followed the caldera collapse after the GT; *ii*) to constrain the petrogenetic relationships between trachytic and pantellerite magmas in order to bind experimentally the parent/daughter relationships; *iii*) to add further constrain on the pre-eruptive conditions of Pantelleria peralkaline rhyolite.

Phase equilibria experiments were carried out for 4 starting compositions (two pantellerites with different (Na+K)/Al ratio and two trachyte) in the pressure range 0.5-1.5 and kbar and temperature range of 750-950 °C. The explored redox conditions were fixed around the FMQ oxygen buffer, maintaining always fluid saturation conditions but exploring different fluid phase composition [$X_{H_2O} = 0-1$ *i.e.* exploring different activities of H_2O (a_{H_2O})] in equilibrium with trachytic and pantelleritic experimental charges.

The experimental results and the comparison with the natural trachyte and pantellerite allowed to add new and valuable constraints regarding: *i*) the storage conditions of trachyte magmas at Pantelleria, and *ii*) the magma differentiation mechanisms and the origin of the different mineral assemblages found in metaluminous to peralkaline rocks with different degrees of evolution.

STARTING MATERIALS

Three target eruptions

The samples studied in this work belong to three eruptive units emplaced during the second and third cycle of volcanic activity at Pantelleria. The oldest unit is the *i*) *Green Tuff eruption*, the last caldera forming eruption at Pantelleria; *ii*) the second eruptive unit is representative of the *post Cinque Denti Caldera magmatism*; *iii*) the third eruptive unit belongs to one of the most energetic eruptive event during the third cycle of activity at Pantelleria, the *Fastuca eruption*. It is worth to note that these three eruptive units cover the last period of activity at Pantelleria (45 to 10 ka) and include the most common eruptive styles at Pantelleria for felsic magmas: *i*) high energy eruption with consequent emplacement of pyroclastic density current, *ii*) violent

strombolian eruption, and *iii*) lava flows. The rocks studied have trachytic and pantelleritic composition and in general they are representative of the felsic pole of Pantelleria rocks. Pantellerites are the most abundant rocks at Pantelleria whereas trachytes, despite the smaller volume erupted, represent the link between the mafic and felsic pole. The petrographic and compositional aspect of the rocks sampled and then used as starting materials for the experiments are described in the sections below.

The Green Tuff basal pumice (GTP)

The pumice composing the Green Tuff basal member presents a high vesiculated texture with crystal content that does not exceeded the 10% in volume. The matrix glass is totally glassy and does not present any microlites whereas the mineral assemblage is dominated (in order of abundance) by alkali feldspar, aenigmatite, clinopyroxene and trace amount of olivine and quartz; rare ilmenite crystal are also presents, in groundmass or included in aenigmatite. Alkali feldspars phenocrysts, with euhedral *habitus* and maximum length of 1 mm, have homogeneous composition $Ab_{65-69}Or_{35-38}$, clinopyroxene are rich in Na and Fe with composition $Wo_{40}En_{10}Fs_{50}$, whereas olivines can be classified as fayalite with composition Fa_{89-93} . Aenigmatites have homogeneous compositions with $X_{Ti} = [X_{Ti} = Ti/(Ti+Fe)] = 0.16-0.17$.

The trachytic member of the Green Tuff (GTT)

The trachytic member of the Green Tuff eruption is constituted by abundant and large (up to 25 mm in length) alkali feldspar phenocrysts, microphenocrysts of clinopyroxene, Fe-rich olivine and Fe-Ti oxides. The groundmass is almost totally crystallised with abundant alkali feldspar and Fe-Ti oxides microlites, whereas clinopyroxene and olivine results rare or absent. Few glass pockets (< 10 vol.%) are present although difficult to be probed. As regards the crystallisation sequence, the textural features highlight a co-precipitation of clinopyroxene and olivine followed by the (large) alkali feldspar phenocrysts, which often enclose other mineral phases originating glomerophyric textures. Alkali feldspars (anorthoclase) phenocrysts show disequilibrium textures, such as resorbed cores and embayments with large corrosion gulfs, sometimes filled by glass.

The Post Cinque Denti Caldera trachyte (PCD)

Textures and minerals composition of the post Cinque Denti Caldera trachyte lavas (erupted from the Mt. Grande-Mt. Gible complex) are similar to the Green Tuff trachyte. Alkali feldspar is the most abundant mineral phase, followed by clinopyroxene, olivine microphenocrysts, and Fe-Ti oxides. Rare amphibole and quartz were found as residual phases in groundmass, which is completely crystallised with alkali feldspar and clinopyroxene microlite. Respect to the Green Tuff member, alkali feldspar does not show deep resorbed or sieved textures but present also oscillatory zoning and patchy textures. The composition of alkali feldspars (anorthoclase) is in the range $An_{03-10}Ab_{65-69}Or_{22-29}$ whereas clinopyroxene and olivine, similarly to the trachyte of the Green Tuff top member, have composition $En_{26-28}Fs_{27-29}Wo_{42-44}$ (with $X_{Fe} = 0.49$) and Fo_{23-27} , respectively.

The Fastuca pantellerite (FP)

Fastuca pumices were sampled in the bottom portion of the fallout deposit. Pumices are dense and, on average, vesiculated. Similarly to other pantellerite, alkali feldspar, clinopyroxene, aenigmatite and trace proportions of fayalitic olivine, ilmenite, and quartz constitute the mineral assemblage; although in small proportion, also amphibole is present in the mineral assemblage as microphenocryst or microlite. The crystal content is close to the 20 vol.% and the most abundant mineral phase, also in this case, is alkali feldspar (15 vol.%), followed by aenigmatite and clinopyroxene, in proportion lower than 5 vol.%. Alkali feldspar tends to form glomerocrystic clots with aenigmatite and clinopyroxene. Clinopyroxene microphenocrysts have compositions $Wo_{43}Fs_{53}En_4$ and $X_{Fe} = 0.93$, whereas amphibole composition varies in the range ferrichterite-arfvedsonite; rare microlite of aegirine are also present in groundmass. Olivines composition is in the range Fa_{90-93} , typical of the olivine found in pantellerites whereas aenigmatite has homogeneous composition with $X_{Ti} = [X_{Ti} = Ti/(Ti+Fe)] = 0.16-0.17$, similarly to the aenigmatite found in the pumice of the Green Tuff basal member.

EXPERIMENTAL METHODS

Starting material preparation

All experiments were performed using as starting material either *i*) a glass prepared from the starting rock or *ii*) a fine powder obtained crushing the natural rock. The initial glass was obtained grounding the natural rock in agate mortar under acetone and then melting the powder in a high temperature furnace at 1300 °C in a platinum crucible, assuming total oxidation. Two melting cycle of 3 hours were realized and, at the end of each cycle, the crucible was rapidly cooled in water in order to obtain a homogeneous glass with the composition of the natural rock.

Experimental equipment

All experiments were carried out in *Internally Heated Pressure Vessel* (IHPV) at Institut des Sciences de la Terre d'Orléans (ISTO) working vertically and pressurized with Ar-H₂ gas mixture. The IHPV allows performing experiments up to temperature of 1300 °C and pressure of 4 kbar. Furthermore, the use of a fixed Ar/H₂ ratio allows imposing variable f_{H_2} within the vessel and consequently it is possible to impose different f_{O_2} within the different capsules loaded in each experiment. The vessel was equipped with an inner furnace (Molybdenum and Kantal furnace) and the temperature was continuously controlled by S-type thermo-couples (± 5 °C of precision) whereas the pressure was recorded by a transducer calibrated against a Heise-Bourdon tube gauge (precision ± 15 -20 bat). The IHPV are also equipped with a fast quench device, which allows a nearly isobaric quench of the experimental charge. Imposing a know Ar/H₂ ratio within the vessel allows to fix the redox conditions within the capsules. The noble metal of the capsule behaves as an ideal semipermeable membrane to H₂, which diffuses relative fast across the membrane and establishing the following equilibrium with the H₂O present in the capsules $H_2 + \frac{1}{2}O_2 \leftrightarrow H_2O$. The equilibrium constant of this reaction at a given temperature and pressure allows knowing the oxygen fugacity (f_{O_2}) if the hydrogen fugacity (f_{H_2}) is known. The f_{O_2} during experiments was indirectly measured ex-post through the *solid sensor technique* (Taylor *et al.*, 1992).

ANALYTICAL TECHNIQUES

Small fragments of experimental products were embedded in epoxy resin and polished carefully. The preliminary studies to identify the mineral phase and the glass portions were carried out using a Scanning Electron Microprobe (SEM-EDS; Cambridge LEO 440) housed at DiSTeM, University of Palermo, and a TESCAN Mira 3 XMU hosted at ISTO. Quantitative analysis of mineral phases and glasses were carried out using an Electron Microprobe CAMECA SX FIVE hosted at CNRS-ISTO; the analytical conditions were: acceleration voltage 15 kV, current 6 nA and counting time 10 s for peak for all elements and 10 s for background.

RESULTS AND DISCUSSIONS

Phase equilibria of Pantelleria trachytes (Italy): constraints on pre-eruptive conditions and on the metaluminous to peralkaline transition in silicic magmas

Recent experimental investigations on both Pantelleria Island and Kenya Rift Valley have laid down the general conditions of storage and evolution of comenditic and pantelleritic magmas at these locations (Di Carlo *et al.*, 2010; Scaillet & Macdonald, 2001, 2003, 2006). However, the parent-daughter relationship between trachyte and pantellerite still awaits experimental investigation. Experiments were performed in the temperature range 750-950 °C, pressure 0.5-1.5 kbar and fluid saturation conditions with XH₂O (= H₂O/H₂O + CO₂) ranging between 0 and 1. Run products include mineral phases, glass and vesicles. The mineral phases identified are clinopyroxene, olivine, feldspar, Ti-magnetite, ilmenite and quartz. The relationships between mineral phases are shown in two projections of direct petrologic use: T-H₂O_{melt} sections (Fig. 1) allow constraining the cooling history of trachytic magma, whereas isothermal P-H₂O_{melt} sections (Fig. 1) show the effect of decreasing P and H₂O_{melt} on crystallization during magma ascent. Phase proportions obtained from mass balance calculations

show that the amount of liquid varies from 98 wt.% to less than 20 wt.%, decreasing with degreasing H_2O_{melt} and temperature.

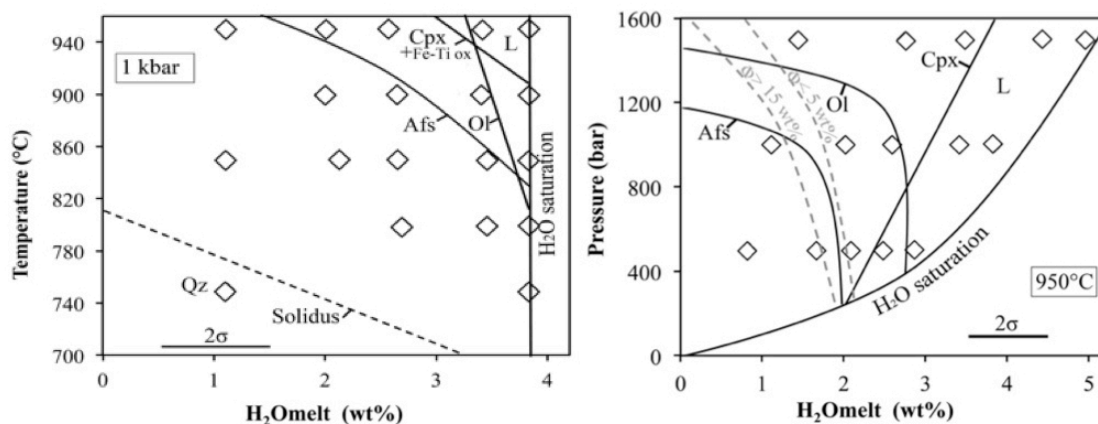


Fig. 1 - Phase relationships of the Green Tuff trachyte in T- H_2O_{melt} projections at 1 kbar (left) and as a function of pressure and H_2O_{melt} at 950 °C (right).

Liquidus conditions were attained at 950 °C and $H_2O_{\text{melt}} \geq 3.5$ wt.% whereas the highest crystal contents (~ 80 wt.%) were obtained at temperatures ≤ 800 °C (Fig. 2). In charges where alkali feldspar does not crystallize, the crystal content never exceeds 12 wt.%. Alkali feldspar, whenever present, increases linearly as the melt fraction decreases, becoming rapidly the dominant mineral phase. At any given temperature and pressure, the amount of alkali feldspar tends to increase with decreasing H_2O_{melt} , but a large increase in alkali feldspar content is also observable when temperature decreases. Clinopyroxene never exceeds 9 wt.% whereas the amount of olivine is usually below 4 wt.%. In charges with alkali feldspar, the afs/(cpx+ol) mass ratio ranges between 4 and 15, increasing when H_2O decreases. These afs/cpx+ol values for experimental charges broadly bracket the value of the natural rocks, which is around 4-6. Fe-Ti oxides proportion ranges between 2 and 5 wt.%. The Green Tuff trachytic phase equilibria were established between 750-950 °C and 0.5-1.5 kbar, whereas for the Post Cinque Denti Caldera Trachyte a more narrow range of temperature (850-950 °C) and pressure (1.0-1.5 kbar) was explored. At 1.5 kbar clinopyroxene is the liquidus phase appearing at 950 °C and $H_2O_{\text{melt}} < 4$ wt.%. At 900 °C clinopyroxene becomes stable at H_2O -saturation at all investigated pressures and is followed by olivine then by alkali feldspar when H_2O_{melt} is lower than 3.5 wt.%. Ilmenite and Ti-magnetite appear at $T < 950$ °C regardless H_2O_{melt} . Clinopyroxene, olivine and Fe-Ti oxide are the liquidus phases at 1 kbar, 950 °C and H_2O_{melt} close to 3 wt.%, followed by alkali feldspar for $H_2O_{\text{melt}} \leq 2.5$ wt.%. Alkali feldspar stability field expands with decreasing temperature, becoming stable at H_2O -saturation at $T \leq 800$ °C. At 0.5 kbar and 950 °C olivine replaces pyroxene as the liquidus phase becoming stable at H_2O -saturation at 900 °C. The isothermal P- H_2O_{melt} projections show that a near-isothermal ascent at either 950 °C or 900 °C promote crystallization and consequently an increase in crystal content with decreasing melt water content.

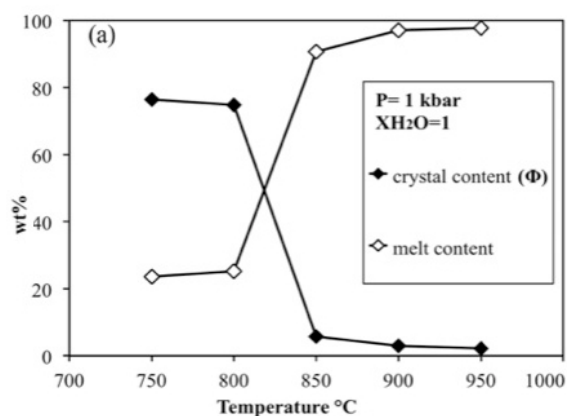


Fig. 2 - Variation of crystal and melt proportions with temperature at 1 kbar and $X_{H_2O} (= H_2O/H_2O+CO_2) = 1$ for GTT experiments.

At 1.5 kbar clinopyroxene is the liquidus phase appearing at 950 °C and $H_2O_{\text{melt}} < 4$ wt.%. At 900 °C clinopyroxene becomes stable at H_2O -saturation at all investigated pressures and is followed by olivine then by alkali feldspar when H_2O_{melt} is lower than 3.5 wt.%. Ilmenite and Ti-magnetite appear at $T < 950$ °C regardless H_2O_{melt} . Clinopyroxene, olivine and Fe-Ti oxide are the liquidus phases at 1 kbar, 950 °C and H_2O_{melt} close to 3 wt.%, followed by alkali feldspar for $H_2O_{\text{melt}} \leq 2.5$ wt.%. Alkali feldspar stability field expands with decreasing temperature, becoming stable at H_2O -saturation at $T \leq 800$ °C. At 0.5 kbar and 950 °C olivine replaces pyroxene as the liquidus phase becoming stable at H_2O -saturation at 900 °C. The isothermal P- H_2O_{melt} projections show that a near-isothermal ascent at either 950 °C or 900 °C promote crystallization and consequently an increase in crystal content with decreasing melt water content.

Experimental clinopyroxenes are augites with composition in the range $En_{26-42} - Fs_{17-58} - Wo_{26-42}$ and X_{Fe} [= $Fe/(Fe+Mg)$, calculated using FeO_{tot}] ranging between 0.27-0.75. Clinopyroxene becomes progressively

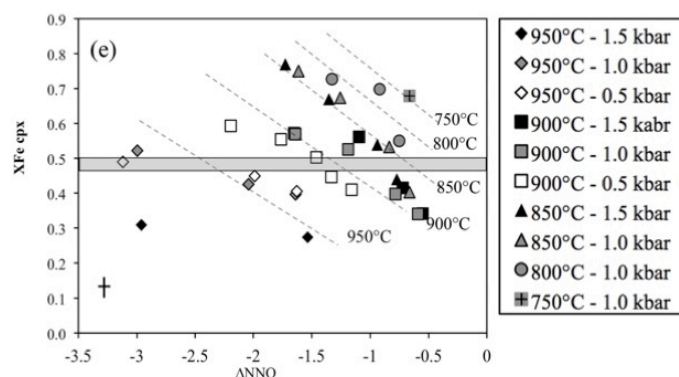


Fig. 3 - Variation of X_{Fe} with oxygen fugacity (expressed as ΔNNO) and H_2O_{melt} in the pressure-temperature range investigated. In all panels the grey box represents the natural clinopyroxene composition while in (c) the white box indicates natural clinopyroxene composition in pantellerites.

richer in Na_2O and FeO_{tot} and poorer in Mg with melt evolution (and hence with decreasing temperature and melt water content). At 950 °C clinopyroxenes have an X_{Fe} ranging between 0.27 and 0.50 while below 850 °C, X_{Fe} reaches values up to 0.75, displaying a good correlation with H_2O_{melt} and fO_2 (Fig. 3). The covariation of $X_{Fe_{tot}}$ with both temperature, fO_2 , pressure and melt water content can be parameterized with the following empirical equation: $X_{Fe} = -0.0024 \times T(^{\circ}C) + 0.0002 \times P(\text{bar}) - 0.2044 \times H_2O_{melt}(\text{wt.}\%) + 0.0718 \text{ NNO} + 3.117$ ($R^2 = 0.92$). The composition of olivine falls in the range $Fo_{46}-Fo_{12}$ [calculated as $Mg/(Fe+Mg+Mn)$] and it can be classified as ferrohortonolite. Olivine composition, as for clinopyroxene, varies systematically with temperature,

H_2O_{melt} and fO_2 , becoming richer in iron content with melt evolution. The more Fe-rich olivine occurs in H_2O_{melt} -poor, or low temperature, charges (*i.e.*, $T < 850^{\circ}C$) where alkali feldspar dominates over clinopyroxene and olivine. Microprobe analyses of alkali feldspar were considered acceptable when the structural formula fulfilled the following criteria: $3.050 < (Si+Al+Fe) < 4.050$ and $0.950 < (Ca+Na+K) < 1.050$ on a 8 oxygen basis. In detail, the An content ranges between 10 mol.% at 950 °C to 2 mol.% at 750 °C while the Or content ranges between 28 mol.% at 750 °C and 20 mol.% at 950 °C, *i.e.* similar to those observed in other compositionally similar systems. At $T \geq 900^{\circ}C$ glass compositions are close to the starting materials, evolving when melt fraction decreases with falling temperature and H_2O_{melt} . Residual liquids are marked by a progressive increase in SiO_2 with respect to the starting material, SiO_2 content ranging between 65 wt.% and 72.8 wt.% in the most crystallized charges. In near-liquidus charges, crystallization of clinopyroxene, olivine and Fe-Ti oxides, produces a decrease in FeO_{tot} and a slight increase in Al_2O_3 . The decrease of temperature and H_2O_{melt} promotes the massive crystallization of alkali feldspar causing a decrease in Al_2O_3 content, which drops from 15.7 wt.% in near liquidus charges down to 11.8 wt.% in crystal-rich charges. Both Na_2O and K_2O tend to remain roughly constant with Na_2O around 5.5-6 wt.% and K_2O at 3.8-4.4 wt.%. Variations in peralkalinity index are thus primarily related to variations in Al_2O_3 content: when melt fraction decreases (*i.e.* at low temperature and low H_2O_{melt}) Al_2O_3 tends to decrease and the peralkalinity index increases up to 1.21 with respect to that of the starting material (0.98). Besides, P-T- H_2O_{melt} , fO_2 changes arising from fH_2O melt variations, also affect the compositions of the experimental mineral phases. Clinopyroxene and olivine compositionally similar to that of the natural trachyte were reproduced in the temperature range 850-950 °C, over a fairly wide range melt water content (1.1 wt.% and 3 wt.%). Combining experimental and petrological results constrains the pre-eruptive condition of Pantelleria trachytic magma at $900 \pm 50^{\circ}C$, 0.5-1.5 kbar, H_2O_{melt} 1-3 wt.% and an fO_2 in the range NNO-0.5 to NNO-2. In our study, phases controlling the trends of glass major elements are clinopyroxene, olivine, Fe-Ti oxides and alkali feldspar, as inferred from the above mentioned geochemical modelling. If we first consider phase proportions, a decrease in temperature from 950 to 750 °C at 1 kbar, increases the crystal content up to 85 wt.%, alkali feldspar being the dominant phase (25-80 wt.% of solids) while the amount of olivine, clinopyroxene and oxides remain lower than 15 wt.%. Considering now the composition of the experimental minerals, with decreasing temperature and fO_2 clinopyroxene have $X_{Fe} > 0.75$ approaching that of

the natural pantellerite ($X_{Fe} > 0.80$), showing also a general Na_2O enrichment. The near liquidus (at 800 °C NNO-1.87) experimental clinopyroxene of Di Carlo *et al.* (2010) has an $X_{Fe} = 0.82$, which is close to that produced after extensive trachyte crystallization in our experiments. Similarly, the olivine crystallizing at 750 °C in trachyte has a fayalitic content (Fa_{83-89}) very similar to that of pantelleritic olivine (Fa_{90}). The decrease in Al_2O_3 is primarily driven by the massive crystallisation of alkali feldspar, whose amount reaches up to 80 wt.% of the crystallizing assemblage at temperatures below 850 °C. As a result, the peralkalinity index of the residual liquid progressively increases as crystallization proceeds, from 0.98 to 1.21, while the Al_2O_3 melt content decreases from 14.8 to 11.8 wt.%. This demonstrates unambiguously, and for the first time, that peralkaline felsic derivatives can be produced from a metaluminous, more mafic, parental magma crystallizing at low pressure.

Crystallisation experiments on two pantellerite starting materials (how small variations in bulk composition and redox conditions influence phase equilibria)

Experimental phase relationships of both pantelleritic starting compositions were established at $P = 1$ kbar and temperature between 900 and 750 °C for the Green Tuff pantellerite and $T = 800-680$ °C for the Fastuca pantellerite. Although the pressure and temperature conditions investigated are similar, the phase diagrams in Fig. 4 differ for the redox conditions imposed during the experiment; for the Green Tuff pantellerite (GTP) they range between ΔNNO -0.5 to -2.5 while for the Fastuca pantellerite (FP) between ΔNNO -1.5 and -2.5. At 1 kbar and 900 °C Green Tuff pumice fall charges are at supra-liquidus conditions regardless the melt water content. At 850 °C clinopyroxene is the liquidus phase for $H_2O_{melt} < 2.5$ wt.% and it is followed by alkali feldspar at H_2O_{melt} close to 1 wt.%. At $T \leq 800$ °C clinopyroxene is liquidus phase at water saturation conditions while alkali feldspar expands its stability field becoming stable when the H_2O_{melt} is close to 4 wt.% at 750 °C. At $T = 800$ °C and H_2O_{melt} around 2.5 wt.% quartz joins the crystallization sequence, whereas aenigmatite becomes stable at 750 °C and $H_2O_{melt} \leq 3$ wt.%. As regard the amphibole, it is stable in all charge at $T < 850$ °C regardless the water content (Fig. 4). The different redox conditions explored for the Fastuca pantellerite arise in some remarkable differences in the phase relationships established by Di Carlo *et al.* (2010) as well as with those of the Green Tuff pantellerite. At 800 °C all charges are at supra-liquidus conditions regardless the water content (Fig. 4).

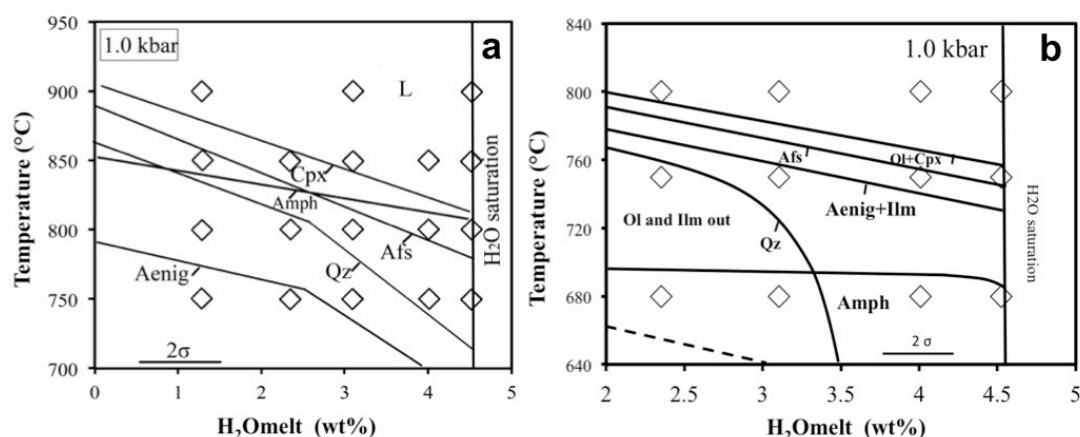


Fig. 4 - a) Phase relationship of the Green Tuff pantellerite (GTP) in the $T-H_2O_{melt}$ section at 1.0 kbar and $f_{O_2} \sim FMQ$. b) Phase relationships of the Fastuca pantellerite (FP) at 1.0 kbar and $f_{O_2} < FMQ$ buffer. L: liquid; Cpx: clinopyroxene; Ol: olivine; Afs: alkali feldspar; Qz: quartz; Ilm: ilmenite; Aenig: aenigmatite. The tick on a phase boundary marks the side on which an experimental phase is stable. Dashed lines are estimated phase boundary.

At $T = 750$ °C clinopyroxene and Fe-rich olivine are the liquidus phase at H_2O_{melt} saturation conditions (~ 4.5 wt.%). For $H_2O_{melt} = 4$ wt.% alkali feldspar joins the crystallization sequence while at 680 °C it becomes

stable at H_2O_{melt} saturation condition. As regards fayalitic olivine and ilmenite, their stability field is limited at 750 °C and for a narrow range of melt water content that is between 3-4.5 wt.% for olivine and 3-4 wt.% for ilmenite (Fig. 5); both disappear when melt water content is lower than 3 wt.%. It is worth to note that, in contrast to the natural rocks, fayalite has not been found coexisting with quartz. Aenigmatite become stable at 750 °C and $H_2O_{melt} \leq 3$ wt.% and together with amphibole remain stable at 680 °C regardless the melt water content. Lastly, quartz crystallizes only when melt water content is lower than 2.5 wt.% at 750 °C or lower than 3.5 wt.% at 680 °C. The amount of liquid varies from 100 to 36 wt.%, decreasing when temperature and melt water content decrease. Supra-liquidus conditions were attained at 900 °C for the Green Tuff pantellerite and 800 °C for Fastuca pantellerite while the highest crystallized charges are those at $T \leq 750$ °C. Decreasing temperature and H_2O_{melt} alkali feldspar become the most abundant mineral phase reaching a mass proportion of 43 wt.% in the most crystallized charges. The application of several thermobarometers based on inter-crystalline (clinopyroxene-olivine), or crystal-liquid exchange equilibria (cpx-liquid, feldspar-liquid) led White *et al.* (2005) to show in detail that peralkaline rhyolites of Pantelleria record temperatures ranging between 680-800 °C and redox conditions in the range ΔFMQ -0.55, -1.06. They reported also different mineral assemblages in pantellerites showing that the main variations in the mineral assemblage regard principally the presence of fayalitic olivine and aenigmatite. In particular, they indicated that fayalite is stable only at low medium peralkalinity index ($NK/A < 1.63$) while when peralkalinity index becomes > 1.75 only aenigmatite (besides alkali feldspar and clinopyroxene) is stable. Furthermore, they showed a strong correlation of mineral assemblage with melt peralkalinity index and whole-rock SiO_2 content, which in turn appears to correlate negatively with T and fO_2 . Di Carlo *et al.* (2010), constraining experimentally temperature and fO_2 , reported pre-eruptive temperatures between 680 and 720 °C and redox conditions around the FMQ buffer confirming both the low temperature evolution and the reduced redox conditions of Pantelleria rhyolites. If we now compare the experimental phase relationships obtained from our experiments on Fastuca pantellerite with those of Di Carlo *et al.* (2010), we observe how an apparently small difference in the redox condition imposed during the experiments have an important impact on the phase topology/relationships of pantellerites. At $T = 800$ °C, indeed, charges of Fastuca starting composition are at supra-liquidus conditions regardless the water content; in the experiments of Di Carlo *et al.* (2010) and also in the experiments on Green Tuff pantellerite, at the 800 °C crystallize in order clinopyroxene, alkali feldspar and quartz. A depression of solidus of ~ 30 °C in peralkaline rhyolite under reducing conditions have been reported by Scaillet & Macdonald (2001), here we document also the effect on liquidus temperature that decrease of ~ 50 °C. Something similar have been observed on metaluminous silicic composition by Dall'Agnoll *et al.* (1999), indeed, they showed a significant decrease in the thermal stability of the tectosilicates at reduced redox conditions. Although from a purely qualitative point of view, it is worth to note that the reason why we were able to analyse the glass composition also in the charge at 680 °C and $X_{H_2O} < 1$, contrarily to Di Carlo *et al.* (2010), is probably related to a further depression of the solidus of pantellerite at more reducing conditions. The variation in fO_2 obviously affects also the Fe^{2+}/Fe^{3+} and hence the iron-bearing phase composition and proportion. In our experiments on Fastuca pantellerite at 750 °C coexist alkali feldspar, aenigmatite and clinopyroxene, *i.e.*, the three most abundant phases in the natural pantellerites, moreover at this temperature also quartz and fayalite can be stable. Fayalite is often found in the mineral assemble of pantelleritic rocks with alkali feldspar, clinopyroxene \pm oxides \pm aenigmatite. In our experiments, we have observed that to crystallize fayalitic olivine the redox conditions has to be close to ΔNNO -1.5. Otherwise, there is not other explanation for non-crystallization of olivine in the experiments of Di Carlo *et al.* (2010) as well as in GT pantellerite. Indeed, liquids with composition compatible with the stability of fayalite and similar water content have been reproduced experimentally both by Scaillet & Macdonald (2003, 2006) and Di Carlo *et al.* (2010) but fayalite has not been synthesized. The fact that at 680 °C even at low redox conditions olivine does not crystallize is probably due to the low temperatures that constitutes a thermal limit to the stability of such a mineral. At temperature lower than 700 °C the mineral that can accommodate large quantity of Fe^{2+} would be the amphibole besides clinopyroxene and aenigmatite. Extrapolating the information

useful to constrain the pre-eruptive redox conditions and temperatures, it worth to note that in the experimental charges at 750 °C and H_2O_{melt} ranging between 3 wt.% and 4.5 the crystal content remain similar to those observed in natural pantellerites, while at 680 °C the crystal content increases from 30 wt.% to 63 wt.% when melt water content decreases. Moreover, as already pointed out by Di Carlo *et al.* (2010), the stability of aenigmatite and now also fayalite could represent the main topological argument to limit the pre-eruptive temperature of pantellerites at 750 °C maximum and redox conditions between ΔNNO -0.5 and -2.0. However, further constraints on pre-eruptive temperature and oxygen fugacity can be gained by comparing the composition of experimental phases with the natural minerals.

Melt inclusions constraints and experimental glass compositions

Water content in Pantelleria rhyolites have been debated for a long time, several researchers have focused their attention on the volatile content dissolved in melt inclusion using different techniques and not always it has been obtained homogeneous results. More in detail, over 80 melt inclusions analysed, the 63.8% of them have water content in the range 2.5-4.5 wt.%, the remnant are out of this range. Interpreting the results of melt inclusions studies in the light of the phase relationship determined experimentally, the melt water contents reported in the recent studies are perfectly compatible with the crystallization of clinopyroxene, alkali feldspar, aenigmatite, olivine \pm amphibole at 750 °C, 1 kbar and fO_2 in the range ΔNNO -0.5 to -2.0. Most of the melt inclusions analysed have been found on alkali feldspar with a quite homogeneous composition ($Ab_{65}-Or_{35}$), which in our experiments crystallizes at 750 °C, 1 kbar and water content 3.5 ± 0.5 wt.%. As already discussed by Di Carlo *et al.* (2010), the fact that composition of alkali feldspar remains almost constant while the H_2O_{melt} decreases, it can explain also the variability in melt water content encountered in melt inclusion trapped in alkali feldspar. Otherwise, the other explanation for those melt inclusions with lower water content is the post entrapment modification. In contrast, those melt inclusion with 4.5 wt.% or slightly higher hosted in alkali feldspar probably have recorded crystallization pressure conditions marginally higher ($\sim 1.2-1.3$ kbar). Indeed, following the phase relationship in Fig. 4 at 1 kbar and 4.5 wt.% of water dissolved in the melt, pantellerites are close or at water saturation conditions and alkali feldspar does not crystallize. Gioncada & Landi (2010) reported also analyses of melt inclusions trapped in olivine and aenigmatite phenocrysts, although statistically less

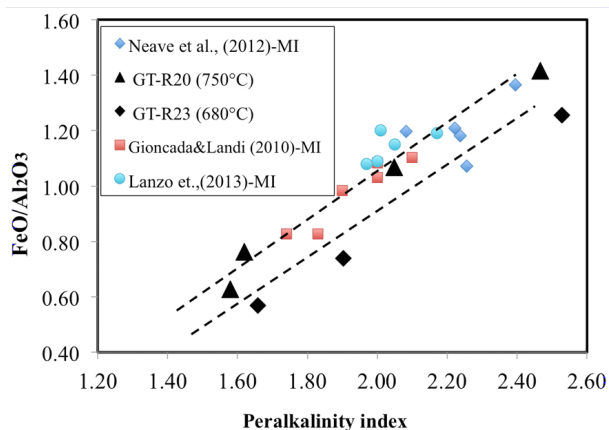


Fig. 5 - Composition of the experimental glasses in the projection FeO/Al_2O_3 vs. the melt peralkalinity of Fastuca pantellerite compared with the composition of natural glasses (Melt inclusions, MI).

significant respect to the data from melt inclusions trapped in alkali feldspar, the water contents found corroborate the crystallization process from a pantelleritic melt with water content between 2.5 and 4.5 wt.%. Indeed, in the melt inclusion trapped in aenigmatite crystals $H_2O = 2.57 \pm 0.1$ whereas in fayalite the highest water content measured is 4.33 wt.%. As regards the water content found in melt inclusions trapped quartz phenocrysts, we support the idea of Di Carlo *et al.* (2010) that a polybaric crystallization is required to explain the low melt water content otherwise the simple water lost upon cooling would increase the crystal content of the magma (over the 30 wt.%) much more of that observed in natural pantellerites. It is important to note that the evolution of the mineral assemblage of Pantelleria rhyolites as function of peralkalinity index has been well reproduced experimentally.

Considering the experimental phases and the glass composition, fayalite is stable when peralkalinity index ranges between 1.58 and 2.05, it coexists also with aenigmatite when the P.I. is around 2 while for higher values (*i.e.*, GT-R20-4; P.I. = 2.47) only aenigmatite is stable; in contrast, in our experiments the SiO_2 content remain

constant around 71.5 wt.%. The important information is that for a similar crystal content, the different mineral assemblages can be originated at the same temperature of 750 °C but a different redox conditions or melt water content. In addition, plotting in a diagram FeO/Al₂O₃ vs. P.I. the experimental glass with natural products such as whole rock and melt inclusions compositions (Fig. 5), the natural products match the experiments at 750 °C. Looking in details to the composition of melt inclusions, most of them are close to that charge in which alkali feldspar, clinopyroxene, olivine and aenigmatite crystallize. This in turn imply that these melt inclusions were trapped when the liquid had already crystallized the four above-mentioned mineral phases, in contrast the composition of melt inclusions trapped in olivine appear less evolved. Lastly, the fact that natural products match with experiments at 750 °C indicates both the evolution temperature at 750 °C and also that amphibole does not fractionate during Pantelleria rhyolite evolution, explaining also why it is found only rarely in the mineral assemblage of pantellerites from Pantelleria.

REFERENCES

- Dall'Agnoll, R., Scaillet, B., Pichavant, M. (1999): An experimental study of a lower Proterozoic A-type granite from the eastern Amazonian craton, Brazil. *J. Petrol.*, **40**, 1673-1698.
- Di Carlo, I., Rotolo, S.G., Scaillet, B., Buccheri, V., Pichavant, M. (2010): Phase equilibrium constraints on pre-eruptive conditions of recent felsic explosive volcanism at Pantelleria Island, Italy. *J. Petrol.*, **51**, 2245-2276.
- Gioncada, A. & Landi, P. (2010): The pre-eruptive volatile contents of recent basaltic and pantelleritic magmas at Pantelleria (Italy). *J. Volcanol. Geoth. Res.*, **189**, 191-201.
- Scaillet, B. & Macdonald, R. (2001): Phase relations of peralkaline silicic magmas and petrogenetic implications. *J. Petrol.*, **42**, 825-845.
- Scaillet, B. & Macdonald, R. (2003): Experimental constraints on the relationships between peralkaline rhyolites of the Kenya rift valley. *J. Petrol.*, **44**, 1867-1894.
- Scaillet, B. & Macdonald, R. (2006): Experimental constraints on pre-eruption conditions of pantelleritic magmas: Evidence from the Eburru complex, Kenya Rift. *Lithos*, **91**, 95-108.
- Taylor, J.R., Wall, V.J., Pownceby, M.I. (1992): The calibration and application of accurate redox sensors. *Am. Mineral.*, **77**, 284-295.
- White, J. C., Ren, M., Parker, D. F. (2005): Variation in mineralogy, temperature, and oxygen fugacity in a suite of strongly peralkaline lavas and tuffs, Pantelleria, Italy. *Can. Mineral.*, **43**, 1331-1347.